Model-Free Precise in-Hand Manipulation with a 3D-Printed Tactile Gripper

Benjamin Ward-Cherrier, Nicolas Rojas, and Nathan F. Lepora

***Abstract*—The use of tactile feedback for precision manipulation in robotics still lags far behind human capabilities. This study has two principal aims: 1) to demonstrate in-hand reorientation of grasped objects through active tactile manipulation; and 2) to present the development of a novel TacTip sensor and a GR2 gripper platform for tactile manipulation. Through the use of Bayesian active perception algorithms, the system successfully achieved in-hand reorientation of cylinders of different diameters (20, 25, 30, and 35 mm) using tactile feedback. Average orientation errors along manipulation trajectories were below 5° for all cylinders with reorientation ranges varying from 42° to 67°. We also demonstrated an improvement in active tactile manipulation accuracy when using additional training data. Our methods for active tactile manipulation with the GR2 TacTip gripper are model free, can be used to investigate principles of dexterous manipulation, and could lead to essential advances in the areas of robotic tactile manipulation and teleoperated robots.**

***Index Terms*—Dexterous manipulation, force and tactile sensing, grippers and other end-effectors.**

I. Introduction

IN-HAND and precision manipulation in humans relies strongly on tactile feedback [1]. Similarly in robots, tactile information is likely essential for any fine manipulation task [2], as it provides clues to the shape, texture, in-hand position and orientation of a grasped object. Many tactile sensors have been developed for integration with robot hands [3]; however complex tactile manipulation (i.e. in-hand repositioning and reorientation of objects through the use of tactile feedback) is still an area in which humans vastly outperform robots.

Our aims in this study are two-fold: 1) To demonstrate in-hand tactile reorientation of grasped objects through in-hand manipulation. 2) To present the novel integration of a tactile sensor and gripper system for tactile manipulation.

Fig. 1. The GR2 gripper with integrated TacTip sensors.

The first aim of tactile reorientation is tested by manipulating cylinders of different diameters along a trajectory of target orientations. Tactile data allows for localization of the object along the manipulation trajectory, while active perception algorithms control the object's orientation, effectively following an in-hand manipulation trajectory.

The second aim of developing a hardware platform for tactile manipulation consists of a novel tactile sensor based on the TacTip [4] which recently demonstrated sub-millimetre localization of objects [5], [6]. Two TacTip sensors are integrated into the GR2 (grasp-reposition-reorient) gripper [7] (Fig. 1). The GR2 gripper is controlled through a shifting position-torque control system and simultaneously repositions and reorients grasped objects. This platform has the potential to investigate principles for dexterous in-hand manipulation.

Overall, we found that accurate reorientation of objects along complex trajectories was successfully achieved through active tactile manipulation (average error in trajectory was below 5° for cylinders of diameters 20, 25, 30 and 35 mm). The amount of training data was also found to influence active manipulation accuracy. For the 20 mm cylinder, average angular error along the manipulation trajectory was $e_\theta = 5.0^\circ$ for 1 training set and $e_\theta = 3.4^\circ$ for 10 sets. Our approach is based on an initial

Manuscript received February 15, 2017; accepted June 3, 2017. Date of publication June 26, 2017; date of current version July 12, 2017. This paper was recommended for publication by Associate Editor J. McInroy and Editor J. Wen upon evaluation of the reviewers' comments. The work of N. F. Lepora was supported in part by a grant from the Engineering and Physical Sciences Research Council (EPSRC) on Tactile Superresolution Sensing (EP/M02993X/1) and a Leadership Award from the Leverhulme Trust on "A biomimetic forebrain for robot touch" (RL-2016-39). The work of B. Ward-Cherrier was supported by an EPSRC DTP studentship. The data used can be accessed in the repositories at http://lepora.com/publications.htm and at the University of Bristol data repository, data.bris, at http://doi.org/b875. *(Corresponding author: Benjamin Ward-Cherrier.)*

B. Ward-Cherrier and N. F. Lepora are with the Department of Engineering Mathematics and the Bristol Robotics Laboratory, University of Bristol, Bristol BS8 1TH, U.K., and also with the University of the West of England, Bristol BS16 1QY, U.K. (e-mail: bw14452@bristol.ac.uk; n.lepora@bristol.ac.uk).

N. Rojas is with the Dyson School of Design Engineering, Imperial College London, London SW7 2AZ, U.K. (e-mail: n.rojas@imperial.ac.uk).

This paper has supplementary downloadable material available at http://ieeexplore.ieee.org.

Digital Object Identifier 10.1109/LRA.2017.2719761

training phase rather than an explicit model of the sensor, gripper or sensor-object interactions, allowing for straightforward generalization to other objects and tactile manipulation tasks. Our methods for model-free active tactile manipulation with the GR2 TacTip gripper can be used to investigate principles of dexterous manipulation and could lead to essential advances in the areas of robotic tactile manipulation and tele-operated robotics.

II. Background and Related Work

The importance of tactile sensing in human manipulation [1], as evidenced by decreased performance in individuals with a lack of tactile feedback as well as the substantial overlap between neural populations involved in tactile sensing and manipulation tasks [8] has led to an interest in tactile sensing in the fields of robotics [9] tele-taction [10] and prosthetics [11]; the aim being to inform human models of perception and perform manipulation tasks with robots. Alongside new hardware developments for tactile sensors [2], the development of perception frameworks such as Bayesian perception [12] have led to control strategies for manipulation inspired by humans [13].

A large number of robotic hands and grippers for manipulation have been developed [14], many of which tend to involve high manufacture costs and complex control systems. The grippers and robotic hands from Yale OpenHand Project [7], [15]–[17] combine a simple fabrication procedure with elegant mechanics to create ideal platforms for investigating in-hand manipulation. Takktile sensors [18] have been integrated in the i-Hy hands [19] for the purpose of object identification [20], however tactile feedback was low resolution (5 taxels per digit) and was not used as a means to affect control of the hand in that study. Previous work by Ward-Cherrier *et al.* [21] investigated the use of a TacThumb, a modified TacTip, on the M2 gripper [17] for the localization of grasped objects. This study aims to extend that work by demonstrating reorientation of a grasped object through in-hand tactile manipulation on a GR2 gripper [7] with integrated TacTips.

The TacTip sensor is an optical, 3d-printed open source tactile sensor developed at Bristol Robotics Laboratory [4]. It differs from previous optical tactile sensors by adopting and tracking biomimetic pins on its inside surface. The compliance of the TacTip is an intrinsic part of its transduction mechanism and renders it ideal to investigate manipulation, as soft sensors have been demonstrated to be more effective than rigid sensors at grasping [22], as well as accurately detecting phase changes in manipulation tasks while maintaining grip [23], [24]. Although studies using model-based approaches to soft finger sensing have been performed [25], we opted for a non-model based method based on running a training phase to construct a likelihood model, following other work on using biomimetic active touch to perceive and explore objects [26], [27].

III. Methods

A. Hardware

The GR2 TacTip is a version of the TacTip that has been miniaturised and adapted for use with the Raspberry Pi 3 (Raspberry Pi, Model 3B) and the GR2 gripper [7]. The hardware setup is an improvement and extension to the TacThumb/M2 Gripper system [21] which now allows for movement of the fingers with integrated TacTips, has a strongly reduced form factor and is integrated on a gripper designed for more elaborate movement [7]. After reviewing the fabrication method and function of the TacTip sensor's design, we list these improvements in more detail below.

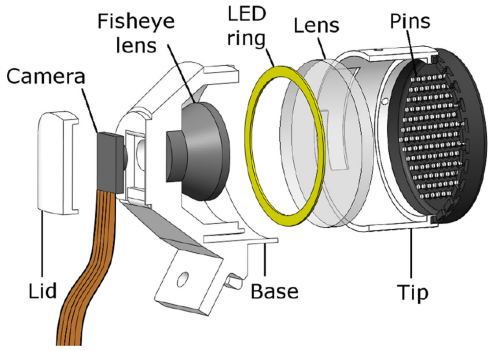

Fig. 2. Design of the GR2 TacTip. The pins on the inside of the base's rubber membrane are illuminated by the LED circuit. These pins are displaced during object contact, and are tracked by an Adafruit Spy Camera with a fisheye lens mounted in the base.

1) TacTip Design Principles: The original TacTip is an optical tactile sensor developed in 2009 at Bristol Robotics Laboratory [4]. It operates by using a camera to track the deflections of biomimetic pins on the inside surface of its outer membrane. These deflections are interpreted as tactile feedback, and are dependent on the contact location, force applied, object shape and texture. The design of the TacTip, like the current GR2 adapted version is comprised of 4 main elements (Fig. 2). The tip contacts objects and is comprised of a rubber-like material skin, with white pins ($\sim$1 mm dia.) on its inside surface. The tip is entirely 3d-printed using a multi-material 3d-printer (Stratasys Objet 260 Connex), with the rigid parts printed in Vero White material and the compliant skin in the rubber-like TangoBlack+. An acrylic lens separates the electronic parts from the tip, filled with RTV27905 silicon gel for compliance. A circuit of 6 LEDs illuminates the rubber pins, which protrude from the tip's inside surface and are topped with circles of white 3d-printed material. Finally the base contains a camera that tracks pin movements when the sensor contacts objects. As with the original TacTip, this sensor is low cost, robust and easy to assemble.

2) The GR2 TacTip: We aim to demonstrate tactile manipulation using the GR2 gripper [7], which introduces some new challenges relative to the previously used M2 gripper [17]. Both fingers of the gripper now move, and the TacTip thus needs to be mounted on a moving finger. To this end, we move towards Raspberry Pi compatible miniature cameras (Adafruit, Spy Camera Module), which are significantly smaller than the Microsoft LifeCam Cinema webcam used previously. This version of the TacTip also features a fisheye lens to enhance the camera's field of view, enabling it to be mounted closer to the skin, and thus strongly reducing the overall form factor of the GR2 TacTip. Dimensions of the GR2 TacTip are 40 mm diameter and 44 mm height (compared to 85 mm for the original

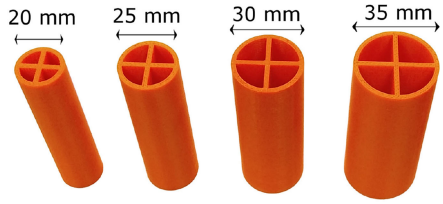

Fig. 3. 3D-printed stimuli used in experiments. Cylinder diameters vary from 20 mm (leftmost cylinder) to 35 mm (rightmost cylinder) in 5 mm increments.

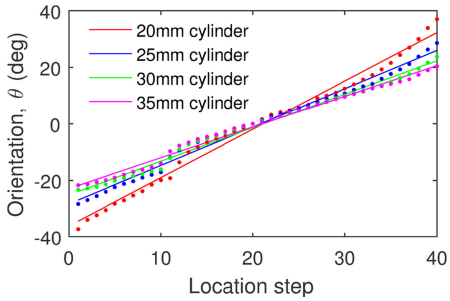

Fig. 4. Orientations at each step location along the gripper's range. Measured orientations are marked with dots, and estimated orientations (using a best line fit) are displayed as lines.

TacTip). We take advantage of the multi-material 3d-printed tips introduced with the TacThumb [21] which allow for easy modification of the tips to flat versions, leaving more room between the gripper's fingers to grasp larger objects.

The GR2 TacTip sensor is mounted on the GR2 gripper [7] (Fig. 1). GR2 stands for grasp-reposition-reorient and the gripper is designed with precision manipulation capabilities allowing in-hand reorientation of grasped objects while maintaining a stable grasp (Fig. 4). Each finger of the GR2 gripper is connected to an MX-28 Dynamixel servo, and rather than use complex control algorithms to calculate finger positions during object manipulation, the fingers are controlled through a combined position-torque control scheme. While one position-controlled finger pushes the object, the other finger uses torque control to maintain a stable grasp. The GR2 includes coupled elastic bands linking fingers to its base link and implementing a passive return, which improves precision manipulation behaviour without affecting grasping performance.

Stimuli used during experiments are cylinders of diameters 20, 25, 30 and 35 mm (Fig. 3), all 3d-printed on a Stratasys Fortus 250MC printer in ABS plastic.

B. Data Collection and Processing

1) Data Collection: The full range of motion of the GR2 gripper (Fig. 4) is separated into 40 discrete positions, with data collected from both TacTips at each position. Object orientation is used as a measure of the object's in-hand location. Orientations are measured with respect to the object's initial grasped position at every location for each stimulus. We measure orientations with an optical tracking method in which the cylinder's inner crossing segments are measured with respect to the horizontal. Each experiment is filmed from above as it runs through its entire location range. The video is then fed into specialized software (Kinovea) in which angle to the horizontal is measured at each position step for each cylinder (Fig. 5). Steps in orientation vary in an approximately linear fashion, and orientations are thus estimated based on measured values using linear regression to obtain a best line fit. The full range of object orientations depends on object size and shape, and here the ranges vary from $-34.4°$ to $32.3°$ for the 20 mm diameter cylinder to $-21.8°$ to $20.6°$ for the 35 mm cylinder.

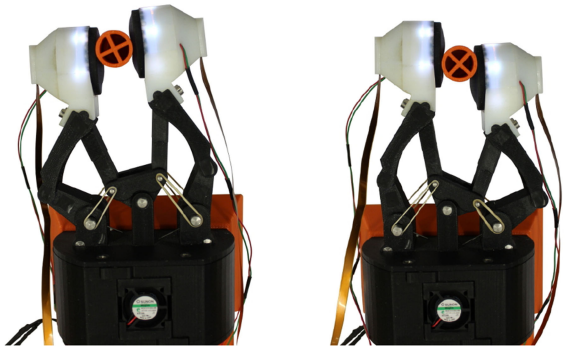

Fig. 5. The GR2 movement range. Grasped objects can be reoriented across a range of orientations. The extent of the orientation range depends on the size of the object (e.g. $-34.4°$ to $32.2°$ for a 20 mm cylinder).

Our experiments are separated into two distinct phases: training, in which data is gathered to form likelihood models representing a particular position and testing, in which data is collected and locations are classified based on training data. We describe the training and testing phases further below.

a) *Training:* During training, cylinders are initially grasped in the centre of the gripper, then brought to its most negative (anti-clockwise) orientation. The object is then reoriented to its most positive orientation in 40 equal increments in motor space (Fig. 4), which will be approximately equal in angle space. The full range of orientations covered is object size-dependent and ranges for the different cylinders are described in the results section.

b) *Testing:* Two forms of testing are implemented. Offline validation gives us an indication of performance (localization accuracy) using cross-validation on pre-collected datasets. Online testing complements this analysis by testing our methods in an active manipulation task to evaluate their performance in a real environment.

In offline validation, both training and testing datasets are collected over the full manipulation range for further analysis. Once the sets have been collected, data is then randomly sampled from the testing datasets using a Monte-Carlo procedure, and used to evaluate algorithm performance.

During online testing, a closed loop between data capture and processing, analysis and the control algorithms for the gripper is implemented. Data is captured in real-time and analysed using the same training sets as for offline validation, followed by an action by the gripper (to follow a given manipulation trajectory).

A supplementary MPEG video clip (2.40 MB) is available at http://ieeexplore.ieee.org and shows the online testing experiment being performed.

2) Data Preprocessing: At each position along the manipulation trajectory, the GR2 TacTip sensors each capture 10 frames at approximately 20 fps. As described in Section III-A2, frames are captured using Raspberry Pi compatible cameras, each connected to a separate Raspberry Pi 3. This data is then streamed through a TCP/IP connection to a desktop computer. It is then pre-processed in Matlab using a series of image processing techniques to reduce noise and find the x- and y-coordinates of the pin centres in each frame.

In order to track pins from frame to frame, and ensure pin identities are maintained throughout the experiment, each pin is compared to the set of pins from the previous frame, and assigned an identity based on its closest pin. We deal with the possibility of missing pins in a given frame by setting a search radius of 20 pixels around each pin. If no corresponding pin is found within that radius in the previous frame, the pin's previous position is used.

3) Passive Location Perception: Passive localization of grasped objects along the manipulation trajectory of the GR2 gripper relies on methods previously applied to the TacTip sensor for superresolution [5] and tactile quality control [6]. A summary of these methods is included here, and we refer to refs [28], [29] for a more detailed explanation. The methods rely on the use of training data rather than explicit models of the gripper and sensor, and can thus be separated into a training phase and a testing phase.

a) *Training* During training, 10 datasets are collected at 40 discrete positions along the manipulation trajectory. Each position is considered a separate location class and a histogram method is used to construct a likelihood model for each class.

b) *Testing:* In the testing phase, the likelihood model is used to determine the log likelihood values of test data at each location. Test data is obtained by collecting 5 distinct datasets and randomly sampling data from these sets using a Monte-Carlo process. We apply maximum likelihood to select the most likely location class from the training data and assign a location decision error for that sample. A mean decision error e_θ for each location class θ is then calculated by averaging errors over all samples for that class.

4) Active Manipulation: Active manipulation requires a shift from open-loop to closed-loop control: object location is actively controlled based on the classification results of incoming tactile data. A manipulation trajectory is first set as a series of objective locations for the gripper to achieve. The gripper moves to its target position and estimates its location as described above. A new target location is then sent to the gripper to move to, which it does relative to its current location belief. The hand thus attempts to follow the defined trajectory over time based solely on tactile feedback.

Location probabilities are updated using Bayes rule during manipulation [5], [28], with previous posteriors used as priors for the current location. Priors are shifted with the gripper's movements to remain aligned with the current location and are combined with sampled likelihoods to obtain probabilities of the current location class.

We report orientation errors in active manipulation as the difference at each location between the target and actual orientation, and use this as a measure of performance of tactile manipulation.

IV. Results

A. Inspection of Data

Training data are initially collected for the 20 mm diameter cylinder. The cylinder is repositioned and reoriented across a range of locations corresponding to the GR2 gripper's range of motion for that object. Orientation of the grasped object is measured with respect to its initial grasped position in the gripper, and this orientation is used to describe the object's location along the manipulation trajectory.

For the 20 mm diameter cylinder, orientation is varied along a 66.7° range (-34.4° to 32.3° relative to the central grasped position) in 40 increments. At each object orientation (also referred to as locations in the manipulation trajectory) we record pin deflections in the x- and y-directions as described previously (Section III-B2). The default pin positions (when no object is grasped) are subtracted from training data to obtain pin deflections in the x- and y-directions. Although training data is considered from both sensors simultaneously, the sensors have been displayed separately for purposes of clarity here (Fig. 6).

Fig. 6 illustrates the deflections of pins from each sensor (panel (a) is for the left finger TacTip, panel (b) for the right) at each of the 40 object locations along the manipulation trajectory. Each pin is identified by colour (rightmost panel), and step changes in deflection correspond to the gripper moving to the next object orientation. Deflections are also separated into their components in the x-direction (top graphs) and y-direction (bottom graphs).

An overall wave-like shape can be observed in the data (Fig. 6), with areas of greater overall pin deflection likely due to increases in grip force from the gripper. These slight variations in force are part of the tactile information captured by the TacTip sensors, and could aid the system in localizing grasped objects.

B. Validation-Object localization

For initial localization validation, we gather 15 datasets over 40 locations with the 20 mm diameter cylinder. 10 of these are considered training sets, and the remaining 5 are used for testing purposes. 10000 data points are sampled randomly from the testing datasets with a Monte Carlo procedure to obtain average localization errors $e_\theta(\theta)$ at each location (Section III-B3).

Additional training datasets are necessary to obtain accurate localization. Running analyses with 1, 5 and 10 training datasets (Fig. 7), shows the correlation between the number of training sets used and localization accuracy. The average localization error over all locations is $e_\theta = 2.1^\circ, 0.7^\circ$ and 0.2° for 1, 5 and 10 training sets respectively. Accuracy is improved with added training sets, however there is a balance to strike between increased training time and improvement in localization (which diminishes with every additional training set). We consider 10 training sets to strike the appropriate balance. Some variation in localization accuracy is also present along the manipulation trajectory with the mid range (-6° to 18°) displaying the

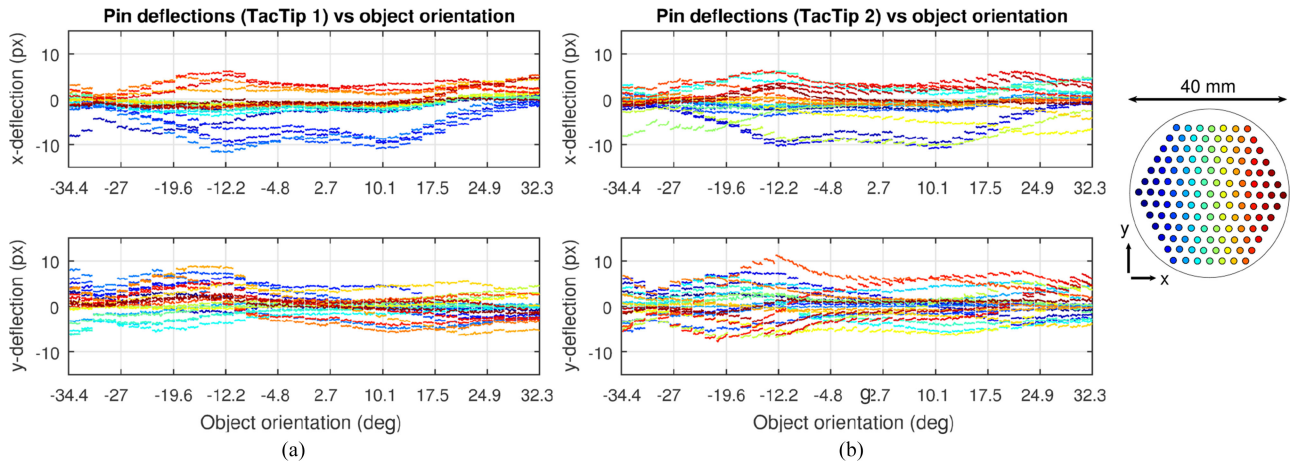

Fig. 6. Training dataset recorded for the 20 mm diameter cylinder. Data from just 22 pins are displayed for clarity purposes and separated into data from the GR2 gripper's left finger in panel (a) and right finger data in panel (b). Within each panel, the top graph represents deflections in the x-direction, and the bottom graph in the y-direction. Pins are identified by color according to the legend in the rightmost panel.

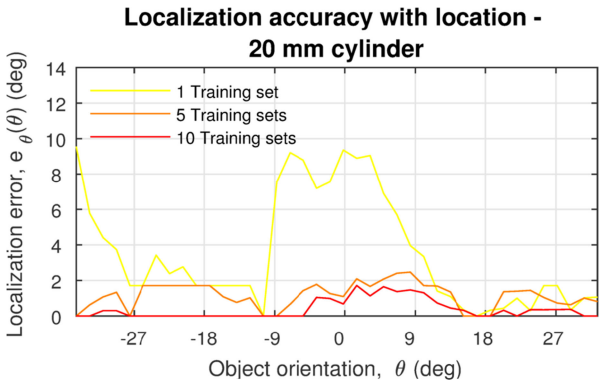

Fig. 7. Localization based on location along the manipulation trajectory and number of training sets used. There is a clear reduction of average localization errors with increased number of training sets.

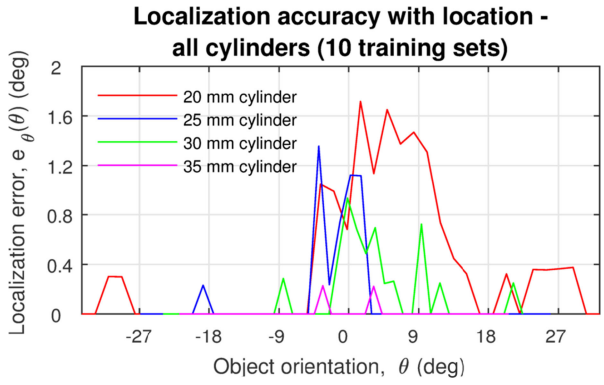

Fig. 8. Localization accuracy based on location for all cylinders (ten training sets each). Localization errors are low overall, but seem to increase around the -6° to 18° region.

TABLE I
ORIENTATION RANGES AND AVERAGE LOCALIZATION ERRORS $\bar{e_\theta}$ FOR ALL CYLINDERS (TEN TRAINING SETS)

Cylinder size	Orientation range	$\bar{e_\theta}$
20 mm	-34.4° to 32.3°	0.4°
25 mm	-26.9° to 26.0°	0.1°
30 mm	-23.9° to 22.4°	0.1°
35 mm	-21.8° to 20.6°	0.0°

highest errors ($e_\theta = 0.3^\circ$ for 10 training sets over that area, which is almost twice the average for the full range). This region is likely not centered within our orientation range due to asymmetries in the gripper control.

We achieved accurate localization using 10 training sets with cylinders of 20, 25, 30 and 35 mm diameters (Fig. 4) over their respective orientation ranges. The GR2 gripper is designed in such a way that the size of a grasped object will affect its range of motion, leading to different orientation ranges for each cylinder, with larger cylinders having more restricted ranges (Table I). Localization errors never exceed 2° for any given cylinder and location, and averages over all locations are below

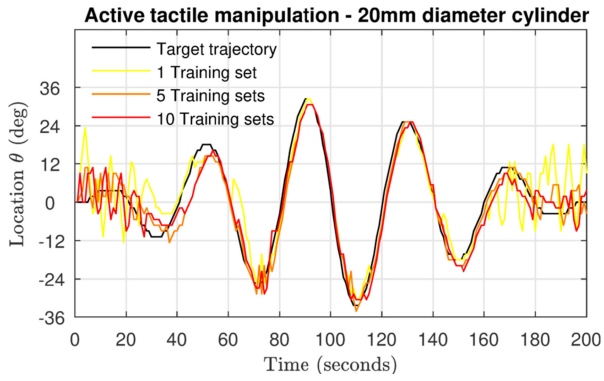

Fig. 9. Active manipulation of the 20-mm cylinder along a sinusoidal trajectory with one, five, and ten training sets. An improved trajectory with additional training data is observable.

0.4° for all cylinders (Table I). Accuracy is moderately higher for larger cylinders with a reduced range of orientations (Table I). Variability in localization is approximately consistent across all cylinders, with the -6° to 18° region displaying the highest errors. This would indicate that tactile information gathered in this region of the manipulation trajectory is less easily distinguishable, regardless of the object grasped.

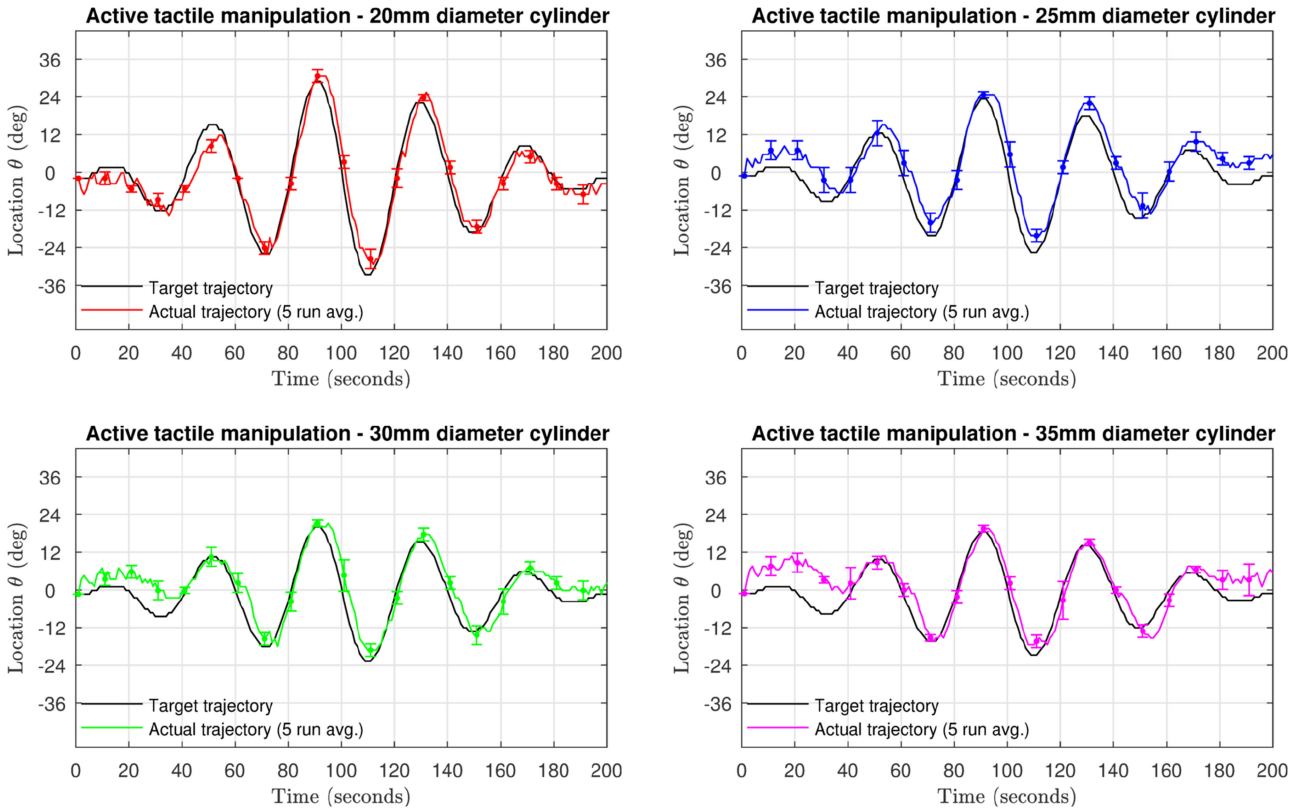

Fig. 10. Active manipulation of the 20-, 25-, 30-, and 35-mm-diameter cylinders. Target trajectories are in black, and actual trajectories followed by the gripper in color. For each cylinder, the average position over five successive runs of the experiment is displayed, with error bars every 10 s showing the standard deviation between runs. We note trajectories are successfully followed for all cylinders, and the centre of the orientation range has increased noise, consistent with our validation results.

C. Active Manipulation

As detailed in the methods section (Section III-B4), active manipulation consists of setting a sequence of target locations along the manipulation trajectory which the GR2 gripper follows through the use of an active control loop. The target trajectory used here spans 200 moves (1 second duration), and is shaped as a sinusoidal with varying amplitude (Fig. 9).

Active manipulation is improved with an increased number of training sets used (Fig. 9). We measure the average trajectory errors as the difference between the target and actual trajectory at each location. With the 20 mm cylinder, we obtain average orientation errors e_θ of $5.0°$, $3.8°$ and $3.4°$ when using 1, 5 and 10 training sets respectively.

Active manipulation is successfully performed with each of the 4 cylinders of varying diameters (Fig. 10). Each graph represents one of the 4 cylinders (20, 25, 30, 35 mm diameter) being tracked and actively reoriented across its given range (Table I), with 10 training sets used in each case. The experiment is performed 5 times for each cylinder (Fig. 10). Orientation errors e_θ over the manipulation trajectories are averaged over each cylinder's 5 runs and reported in Table II. Minor variability exists between cylinder sizes, but all average errors over the full range are kept below $5°$.

There is observable noise present in the centre of the orientation space ($-12°$ to $12°$) for all cylinders (Fig. 10), which is expected based on the lower localization accuracy around that range (Fig. 8). We hypothesize that training data gathered in this region has lower variations in torque and location of the grasped object on the sensor surface (Fig. 6) rendering localization and manipulation more challenging. An important aspect to these trajectories is that noise is strongly reduced towards the end of the trajectories (last 30 loc.) relative to the beginning (first 30 loc.), as shown in Table II. Since trajectories are symmetrical in time, this demonstrates an improvement in performance as more test data is collected, a consequence of our use of Bayesian update algorithms.

TABLE II
ORIENTATION ERRORS FOR ALL CYLINDERS (TEN TRAINING SETS) OVER THE FULL TRAJECTORY RANGE, THE FIRST 30 LOCATIONS OF THE TRAJECTORY, AND THE LAST 30 LOCATIONS

Cylinder size	e_θ - Full range	e_θ - First 30 loc.	e_θ - Last 30 loc.
20 mm	$3.9° \pm 0.2°$	$4.4° \pm 0.4°$	$2.9° \pm 0.5°$
25 mm	$4.8° \pm 0.2°$	$3.9° \pm 0.5°$	$3.9° \pm 0.5°$
30 mm	$4.2° \pm 0.2°$	$4.8° \pm 0.5°$	$1.3° \pm 0.4°$
35 mm	$4.3° \pm 0.2°$	$7.5° \pm 0.6°$	$1.1° \pm 0.8°$

D. Object Placement

To explore how the tactile GR2 gripper system deals with uncertainty in object placement, we rerun the tactile manipulation experiment with the 20 mm cylinder, varying initial position along the an axis emanating perpendicularly from the gripper's

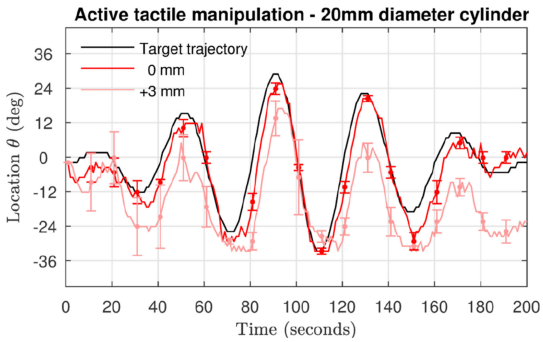

Fig. 11. Active manipulation of the 20-mm cylinder along a sinusoidal orientation trajectory with initial placement at 0 mm and +3 mm along the z-axis relative to the training data. The trajectory is most accurately followed with no displacement between training and testing, however both cases follow roughly sinusoidal trajectories.

TABLE III
AVERAGE LOCALIZATION ERRORS FOR THE 20-MM CYLINDER OVER FIVE EXPERIMENT RUNS WITH INITIAL DISPLACEMENT ALONG THE GRIPPER'S AXIS

Placement	−3 mm	−1.5 mm	0 mm	+1.5 mm	+3 mm
$\bar{e_\theta}$ (°)	20.2° $\pm 0.5^\circ$	13.4° $\pm 0.4^\circ$	5.7° $\pm 0.2^\circ$	7.9° $\pm 0.3^\circ$	16.7° $\pm 0.5^\circ$

palm (which we name z axis) from −3 mm to +3 mm in 1.5 mm increments. Negative displacements along the z axis correspond to a move towards the gripper's palm and positive away from the palm. Positions are varied along the z axis since small variations across this axis would likely result in the gripper displacing the cylinder and automatically correcting its position. Position along the axis is thus easier to control experimentally, and less likely to be solved by the gripper's intrinsic mechanics.

As previously, the experiment is run 5 times at each initial placement and averages over the 5 runs are displayed in Fig. 11 for the 0 and +3 mm displacement cases for comparison purposes. Results for other displacements are summarised in Table III, however we do not display all trajectories in Fig. 11 for purposes of clarity. As expected, the case with 0 mm displacement between training and testing phases of the experiment follows the trajectory most accurately. The +3 mm displacements still maintain a roughly sinusoidal shape, with a systematic shift in orientation corresponding to the direction of initial misplacement. Thus negatively displaced trajectories lie above the target (gripper tends to rotate the object to the left), and positively displaced ones lie beneath it (gripper tends to the right).

Table III shows us the scaling of average orientation errors for trajectories in which we varied initial cylinder placement. As expected, manipulation becomes less accurate the more we initially displace the cylinder (from 5.7° at 0 mm to 20.2° at +3 mm). The spread of trajectories also increases as displacement is increased, as suggested by the trajectory uncertainties (from $\pm 0.2^\circ$ at 0 mm to $\pm 0.5^\circ$ at ±3 mm). There is a slight asymmetry in performance, which suggests the gripper handles displacement better when it is further away from the palm rather than closer (20.2° at −3 mm compared with 20.2° at +3 mm).

V. DISCUSSION

This study describes the successful implementation of model-free active tactile manipulation on a novel tactile gripper. The platform for manipulation consists of two TacTip sensors integrated on a GR2 gripper [7]. We demonstrated this system is capable of performing precise reorientation of grasped objects of different sizes along given gripper trajectories using only tactile feedback. Tactile information was used to adjust the object's orientation based on previously collected training data without an explicit model of the gripper or sensor kinematics and average orientation errors over the manipulation trajectory were kept below 5° for all cylinders.

We also showed the improvement in active tactile manipulation performance when using additional training datasets. This was demonstrated with the 20 mm diameter cylinder (reduction of average error from $e_\theta = 5.0^\circ$ for 1 training set to $e_\theta = 3.4^\circ$ for 10 sets). Initial misalignment of objects within the gripper was explored and we found errors increased rapidly with object displacement, reaching 20° for 3 mm displacement towards the gripper's palm. However trajectories were still approximately followed, albeit with a constant angular displacement throughout the manipulation trajectory, leading to the increased overall errors in active manipulation. The method's robustness to object placement could be improved with further training over a series of initial positions.

Our approach is based on the influential neuroscience theory of perception as Bayesian inference [30], a framework for biomimetic active touch [31] that combines perception via Bayesian evidence accumulation with control of the gripper through perceived object location. This evidence accumulation over the manipulation trajectory explains the improvement in performance towards the end of experiments relative to the beginning. The central part of orientation space displays larger amounts of noise than other areas, and ways to reduce this noise could include gathering further training datasets and fine-tuning control of the gripper around that region.

A further extension to this work would involve the addition of object recognition within the perception algorithm. This would allow the gripper to perform simultaneous object localization and identification [28] of objects being manipulated, creating a more versatile and autonomous gripper. Objects of different shapes, sizes or textures could thus be manipulated by identifying them and associating them with their corresponding training dataset.

The TacTip is a low-cost, robust and easily adaptable tactile sensor. As such, it would be straightforward to investigate the effect of its shape and size on manipulation capabilities. This work could also be further extended by adapting the TacTip for use on more complex robotic hands, such as the OpenHand Model O, an open-source variant of the i-Hy hand [19]. More complex manipulation trajectories will present challenges, and it may be necessary to separate tactile feedback into more precise features such as contact location, force, torque and slip. 3-fingered systems would also increase the amount of data to be processed, potentially requiring optimization of the image processing methods.

Our methods for model-free active tactile manipulation on the GR2 TacTip gripper platform can be used to investigate principles of dexterous manipulation and could lead in future to essential advances in the areas of robotic tactile manipulation and tele-operation.

VI. Conclusion

Active tactile manipulation of grasped objects of different dimensions was achieved with the GR2 gripper and two integrated TacTip sensors. Objects were manipulated along a target trajectory using only tactile feedback, demonstrating precise active manipulation in a manner that could be extended to other tactile manipulation tasks.

Acknowledgment

The authors would like to thank Raymond R. Ma, Luke Cramphorn, Nicholas Pestell, Kirsty Aquilina, and John Lloyd for help with this work.

References

[1] R. Johansson and R. Flanagan, "Coding and use of tactile signals from the fingertips in object manipulation tasks," *Nature Rev. Neurosci.*, vol. 10, no. 5, pp. 345–359, 2009.

[2] R. Dahiya, G. Metta, M. Valle, and G. Sandini, "Tactile sensing—From humans to humanoids," *IEEE Trans. Robot.*, vol. 26, no. 1, pp. 1–20, Feb. 2010.

[3] Z. Kappassov, J-A. Corrales, and V. Perdereau, "Tactile sensing in dexterous robot hands," *Robot. Auton. Syst.*, vol. 74, pp. 195–220, 2015.

[4] C. Chorley, C. Melhuish, T. Pipe, and J. Rossiter, "Development of a tactile sensor based on biologically inspired edge encoding," in *Proc. Int. Conf. Adv. Robot.*, 2009, pp. 1–6.

[5] N. Lepora and B. Ward-Cherrier, "Superresolution with an optical tactile sensor," in *Proc. IEEE Int. Conf. Intell. Robots Syst.*, 2015, pp. 2686–2691.

[6] N. Lepora and B. Ward-Cherrier, "Tactile quality control with biomimetic active touch," *Robot. Autom. Lett.*, vol. 1, no. 2, pp. 646–652, 2016.

[7] N. Rojas, R. Ma, and A. Dollar, "The GR2 gripper: An underactuated hand for open-loop in-hand planar manipulation," *IEEE Trans. Robot.*, vol. 32, no. 3, pp. 763–770, Jun. 2016.

[8] A. Goodwin and H. Wheat, "Sensory signals in neural populations underlying tactile perception and manipulation," *Annu. Rev. Neurosci.*, vol. 27, pp. 53–77, 2004.

[9] H. Yousef, M. Boukallel, and K. Althoefer, "Tactile sensing for dexterous in-hand manipulation in robotics—A review," *Sens. Actuators A, Phys.*, vol. 167, no. 2, pp. 171–187, 2011.

[10] D. Caldwell and C. Gosney, "Enhanced tactile feedback (tele-taction) using a multi-functional sensory system," in *Proc. IEEE Int. Conf., Robot. Autom.*, 1993, pp. 955–960.

[11] M. Tiwana, S. Redmond, and N. Lovell, "A review of tactile sensing technologies with applications in biomedical engineering," *Sens. Actuators A, Phys.*, vol. 179, pp. 17–31, 2012.

[12] D. Knill and W. Richards, *Perception as Bayesian Inference*. Cambridge, U.K.: Cambridge Univ. Press, 1996.

[13] J. Romano, K. Hsiao, G. Niemeyer, S. Chitta, and K. Kuchenbecker, "Human-inspired robotic grasp control with tactile sensing," *IEEE Trans. Robot.*, vol. 27, no. 6, pp. 1067–1079, Dec. 2011.

[14] A. Bicchi, "Hands for dexterous manipulation and robust grasping: A difficult road toward simplicity," *IEEE Trans. Robot. Autom.*, vol. 16, no. 6, pp. 652–662, Dec. 2000.

[15] A. Dollar and R. Howe, "The highly adaptive SDM hand: Design and performance evaluation," *Int. J. Robot. Res.*, vol. 29, no. 5, pp. 585–597, Dec. 2010.

[16] R. Ma, L. Odhner, and A. Dollar, "A modular, open-source 3D printed underactuated hand," in *Proc. IEEE Int. Conf. Robot. Autom.*, 2013, pp. 2737–2743.

[17] R. Ma, A. Spiers, and A. Dollar, "M2 gripper: Extending the dexterity of a simple, underactuated gripper," in *Proc. IEEE Int. Conf. Reconfigurable Mech. Robot.*, 2015, pp. 795–805.

[18] Y. Tenzer, L. Jentoft, and R. Howe, "Inexpensive and easily customized tactile array sensors using MEMS barometers chips," *IEEE Robot. Autom. Mag.*, vol. 21, no. 3, pp. 89–95, 2014.

[19] L. Odhner *et al.*, "A compliant, underactuated hand for robust manipulation," *Int. J. Robot. Res.*, vol. 33, no. 5, pp. 736–752, 2014.

[20] M. Liarokapis, B. Calli, A. Spiers, and A. Dollar, "Unplanned, model-free, single grasp object classification with underactuated hands and force sensors," in *Proc. IEEE Int. Conf. Robots Syst.*, 2015, pp. 5073–5080.

[21] B. Ward-Cherrier, L. Cramphorn, and N. Lepora, "Tactile manipulation with a tacthumb integrated on the open-hand M2 gripper," *Robot. Autom. Lett.*, vol. 1, no. 1, pp. 169–175, 2016.

[22] L. Natale and E. Torres-Jara, "A sensitive approach to grasping," in *Proc. 6th Int. Workshop Epigenetic Robot.*, 2006, pp. 87–94.

[23] K. Shimoga and A. Goldenberg, "Soft robotic fingertips Part 1: A comparison of construction materials," *Int. J. Robot. Res.*, vol. 15, no. 4, pp. 320–334, 1996.

[24] D. Hristu, N. Ferrier, and R. Brockett, "The performance of a deformable-membrane tactile sensor: Basic results on geometrically-defined tasks," in *Proc. IEEE Int. Conf. Robot. Autom.*, 2000, vol. 1, pp. 508–513.

[25] T. Inoue and S. Hirai, "Modeling of soft fingertip for object manipulation using tactile sensing," in *Proc. IEEE Int. Conf. Intell. Robots Syst.*, 2003, vol. 3, pp. 2654–2659.

[26] N. Lepora, "Biomimetic active touch with fingertips and whiskers," *IEEE Trans. Haptics*, vol. 9, no. 2, pp. 170–183, Apr.–Jun. 2016.

[27] N. Lepora, K. Aquilina, and L. Cramphorn, "Exploratory tactile servoing with active touch," *IEEE Robot. Autom. Lett.*, vol. 2, no. 2, pp. 1156–1163, Apr. 2017.

[28] N. Lepora, U. Martinez-Hernandez, and T. Prescott, "Active bayesian perception for simultaneous object localization and identification," in *Proc. Robot.: Sci. Syst. Conf.*, 2013, p. 19.

[29] N. Lepora, U. Martinez-Hernandez, M. Evans, L. Natale, G. Metta, and T. Prescott, "Tactile superresolution and biomimetic hyperacuity," *IEEE Trans. Robot.*, vol. 31, no. 3, pp. 605–618, Jun. 2015.

[30] N. Lepora, J. Sullivan, B. Mitchinson, M. Pearson, K. Gurney, and T. Prescott, "Brain-inspired Bayesian perception for biomimetic robot touch," in *Proc. IEEE Proc. Int. Conf. Robot. Autom.*, 2012, pp. 5111–5116.

[31] N. Lepora, U. Martinez-Hernandez, and T. Prescott, "Active touch for robust perception under position uncertainty," in *Proc. IEEE Int. Conf. Robot. Autom.*, 2013, pp. 3020–3025.